EMITTANCE STUDIES FOR HEAVY ION LINAC

BY

S. JORNA
R. JANDA

THIS EFFORT SUPPORTED BY
ARGONNE NATIONAL LABORATORY
UNDER CONTRACT 31-109-38-5049

PHYSICAL DYNAMICS, INC.
LA JOLLA, CA. 92038

1. Summary

Our three-dimensional linear accelerator code has been applied to calculate transverse and longitudinal phase space dilution for beams of Xe^+ ions carrying average currents in the 15 to 25 mA range. The calculations have been confined to a FOFODODO Wideroe structure operating in the π-3π mode[1] generally with a gap voltage gradient of 5 MV/m; but we have also considered the effect on emittance growth of lowering the gap fields. The r.f. wavelength is 2400 cm, the synchronous phase is -32^{o}, and the quadrupole fill factor ranges from 50-60 percent. The quadrupole lengths are $\beta_s\lambda$ and the magnetic field gradient is varied with the synchronous particle momentum to keep $\int B'dz$ essentially constant. The magnitude of the field gradient is fixed by stability requirements. These then also set the maximum phase spread. Typical beam parameters are: normalized transverse emittance $\gamma\beta_s\varepsilon_t$ = 0.3mm mrad, longitudinal emittance 10^{-4} cm, $\beta_{initial}$ = 0.0061.

The code has usually been run for 160 particles distributed in the transverse phase-space as a K-V distribution. Provided the mesh for the space charge calculations is chosen carefully, this number appears to be entirely adequate for parametric studies. Once matched beam parameters have been found, a 1000-particle case is run, and one typically finds that the emittances are 20-25 percent below those for the 160-particle case. Our experience has been that very little further change results when more than 1000 particles are used. Collective modes which might render the beam unstable cannot be studied with such small particle numbers but they are probably not important here due to the phase mixing in the gaps.

With the focusing gradient and phase spread of the beam set by the stability conditions, the equilibrium beam radius, R, say, is then also determined (by the matching requirement). The calculations show that as a general rule the emittance increases rapidly in the first cell. The perveance

$K = 4.9 \times 10^{-10}\ I(A)/\beta^3$ for Xe^+ ions; I(A) is the current in amperes. Thus the beam is space charge dominated for the emittance considered here at I = 25 mA, $\beta = 0.0061$. The matched radius for a quadrupole gradient $g = 0.031/\beta$ KG/cm turns out to be about 2.4 cm and the transverse emittance grows rapidly by a factor of 3.7. Thereafter, the emittance continues to increase slowly due to a combination of the space charge forces, nonlinear transverse-longitudinal coupling in the gaps, and mismatch due to the finite bunch length. Scatterplots of the particle distribution in the phase spaces indicate that dilution takes place due to the latter effect, but it does not appear to be the dominant contribution.[2] This has been substantiated by code calculations in which the beam was given zero spread. For the 25 mA beam the normalized emittance for a final particle energy of 8.4 MeV increases by a factor of 8 for 100 percent of the particles and by about 6 for 80 percent of the particles. For 15 mA the initial matching radius is about 1.8 cm, and the emittance for a final energy of 8.4 MeV increases for 100 percent of the particles by a factor 5; for 90 percent of the particles the envelope radius is held to a little over 2 cm and the emittance increases by about 4.5. The gain in longitudinal emittance ranges from 3 for 15 mA to 4 for 25 mA.

We have also studied the extent to which emittance increase can be curtailed by lowering the gap fields. For a 25 mA beam, lowering the gap field from 5 to 4 MV/m results in a 20 percent reduction in transverse emittance growth for 80 percent of the particle number when the results are compared at a final particle energy of 7 MeV; from 5 to 2.5 MV/m the reduction is almost 50 percent. For 15 mA the corresponding reduction is about 15 percent in going from 5 to 4 MV/m. Also, 90 percent of the particles are contained with a 2 cm radius, and about 10 percent of the particles are lost from the

"bucket" because of the increased influence of the space charge. The 2 cm limit on the radial excursion does not mean that these results are recovered when particles reaching beyond 2 cm along the accelerator are discarded. This is because particles which are beyond 2 cm at one point will be within this radius further along. The case with a physical stop of a given radius will be considered separately.

The gap defocusing forces will also be reduced by operating with a smaller phase angle, although the space charge forces will then be increased for a given current due to the reduced phase spread, and the accelerator efficiency will suffer if the separatrix length is less than the spread allowed by the stability limits.

In the remainder of this report we discuss these matters in greater detail. Section 2 contains a description of the phenomena which limit the allowable parameter range for beam and accelerator. In Section 3 we present the emittance calculations for some typical beam parameters and the Wideroe structure mentioned above.

2. Constraints

There are two constraints on the length of the bunch. One is set by the separatrix length and is given approximately by the inequalities

$$(1 - S)\phi_s < (\phi - \phi_s) < -2(1 - S)\phi_s \quad ,$$

where S is the ratio of the defocusing space charge to the accelerating force:

$$S = M2\rho\beta_s\lambda/E \sin \phi_s \quad ,$$

where ρ is the space charge density in the bunch, E the r.f. amplitude of the accelerating field, λ its wavelength. The proportionality constant M, whose magnitude ranges from 0 to 1, is determined by the shape of the bunch.

The other is governed by the magnetic focusing stability limits determined by the condition that "μ" be real. For E_{gap} = 5 MV/m and a magnetic fill factor of 50 percent, these limits are for the Wideroe under discussion given by Figure 1 (in the absence of space charge). Here,

$$-\Delta = -0.001294\ E_{gap}(MV/m) \sin \phi \ ,$$

is the strength of the thin lens representing the gap field and g^2 is the square of the quadrupole gradient in kG/cm. The magnetic field gradient is chosen such that for $\phi = \phi_s$ the operating point lies at $\mu = \pi/2$. The maximum phase spread then follows from the range in ϕ which keeps $-\Delta$ between the cos $\mu = \pm 1$ lines. Because instability is due to overfocusing and space charge corresponds to reduced focusing, this should also be the stable regime for non-zero currents. For E_g = 5 MV/m, we find that a focusing gradient of 5.1 kG/cm is required, while for E_g = 4 MV/m this is reduced to 4.9 kG/cm. For the former case, the maximum range in ϕ is $\phi \tilde{-} \phi_s \pm 18^o$ as ϕ ranges from -50^o to -13^o. The maximum phase spread $(\phi - \phi_s)m = (3/2)(1 - S)|\phi_s|$ imposes

the following relation between S and the current (λ = 2400 cm)

$$\frac{1}{4} \geq S(1 - S) \geq 0.049 \frac{I(mA)M}{a_x a_y E(MV/m)} ,$$

where the geometric factor is a function of S and set by the ratio of the mean transverse bunch dimension to its half-length. For $(a_x a_y)^{1/2}/(z - z_s)_m$ = 1.8, the maximum value of $S(1 - S)/M \simeq 0.4$ for $S \simeq 0.4$. Thus, the maximum transportable current $I_{max}(mA) \simeq 8.1 a_x a_y E(MV/m)$ or with $(z - z_s)_m$ = 0.7 cm $I_{max} \simeq$ 13 mA for E = 1 MV/m. The maximum bunch length is set by ϕ_s and S.

If the transverse beam dimensions are greater than the bunch length, the optimum value of S is relatively constant at 0.4. Thus, the maximum theoretical bunch length set by these considerations is about 2.3 cm corresponding to ϕ ranging from -51.2^o to 6.4^o. The phase range permitted by the magnetic stability limits is within these limits, corresponding to a bunch length of about 1.5 cm. Thus, adopting $(z - z_s)$ = 0.7 cm would appear to be conservative.

To determine how stringent the current limit of 13 mA is requires a more precise determination of the space charge forces and the effect of applying acceleration only in the gaps. The actual transverse beam dimension will, of course, be determined by the matching conditions.

Rather than adopting the envelope equations to obtain the matched beam parameters, we have found it expeditious to start from the matched parameters for zero current (obtained from a separate matrix code) and then to increase the current while keeping the beam matched. One only needs to use a few particles and run the code out to a few periods, paying particular attention to the symmetry points. This has the advantage over the envelope equation approach that a K-V distribution need not be assumed and the emittance is not assumed constant. Convergence to the desired optimum parameters is fast so

that automating this search is a practical possibility. In the occasional event that this process becomes tedious, a matrix code is used with space charge and gap defocusing forces represented by delta functions in the gaps. The changing values for β are predetermined in this case.

3. Results

To reiterate, most of our calculations have been run for the following parameters: particle number: 160; initial β: 0.0061; input normalized emittance: 0.32 mm mrad; bunch length: 1.4 cm; initial velocity dispersion: 1 percent; magnetic fill factor: 50 percent; synchronous phase: -32^{o}; magnet arrangement: ++--; accelerating mode: π-3π; gap length: 0.2 $\beta\lambda$.

The injection point has for simplicity been chosen halfway between the x-focusing magnets: the phase-space ellipses are upright here and x and y have extremal values.

To ensure that no spurious emittance growth is generated, a matched beam was passed through the accelerator at zero current. The matching parameters were obtained from a separate matrix code in which the gap acceleration was simulated by thin lenses in the middle of the gaps. The results show that the equations and the difference scheme clearly preserve the normalized emittance.

Unless otherwise stated, the emittances referred to in this paper are normalized r.m.s. values calculated from the relations

$$\varepsilon_x = \beta \left\{ \overline{x^2}\ \overline{x'^2} - \overline{xx'}^2 \right\}^{1/2}, \quad \varepsilon_y = \beta \left\{ \overline{y^2}\ \overline{y'^2} - \overline{-yy'}^2 \right\}^{1/2},$$

$$\varepsilon_z = \left\{ \overline{(z - z_s)^2}\ \overline{(\beta - \beta_s)^2} - \overline{((z - z_s)\ (\beta - \beta_s))}^2 \right\}^{1/2}.$$

These quantities are exactly preserved in linear systems. They have the further advantage of allowing in an r.m.s. sense for non-uniform distribution. The normalizing factor of 1/4 for the K-V distribution assumed here should be kept in mind when comparing absolute values for the emittance with those obtained from uncorrelated distributions. Also, although for 100 percent

transmission our calculated emittances are just those usually referred to as r.m.s. emittance, the emittances for smaller fractions of the beam are determined with reference to a circular hole transmitting a particular percentage of the total number of particles in the beam. To avoid confusion in comparing our results with other calculations these quantities might be more appropriately referred to as transmitted emittances.

Results for I = 15 mA and 25 mA are given in Figures 2 and 3. The curves represent 60, 70, 80 and 100% of total particle numbers, a fifth curve represents 90%. In the legend on each figure, I represents the current (in Amp); x, xp, y and yp represent the input values for the transverse beam dimensions and the envelope gradients (in cgs units). The quantity AL1 is a measure of the magnet fill factor, g is the initial guadrupole gradient in kG/cm, and

$$CCS = 2eE_{gap} \cos \phi_s / Am_1c^2$$

$$= 1.38 \times 10^{-7} E_{gap}(MV/m) \text{ for } Xe^+ \quad .$$

Since ε_x and ε_y remain about equal, we give only plots of their geometric mean. The scales are compatible with the accuracy of these calculations.

It will be noted that if the beam envelope radius is to be kept below 2 cm, 20 percent of the particles will be lost for I = 25 mA, while almost 90 percent will pass for 15 mA. A physical stop will be imposed later; we examine first the idealized case. The emittance increase is also substantially less for the lower current (cf., Figure 5). As we have already noted, much of the emittance adjustment occurs in the first period ($\sim$120 cm) with a continually decreasing rate of increase thereafter. There should therefore be little emittance increase in the second and third tanks if the matching can be preserved.

Emittance is only a crude indication of beam quality and a better representation can be obtained from a scatter plot giving the distributions of the macro-particles in phase space and real space. An example is Figure 4 for I = 25 mA and 320 particles. This case corresponds closely to that of Figure 3, except that a slightly smaller value of Y was used. The quantity z on these graphs is the distance along the accelerator. It is particularly interesting to note the progressive deterioration of the beam in the x - x' and y - y' phase-spaces, and the emittance dilution at z = 695.3 cm represented by the appearance of four wings is apparent. It is also clear that beam match cannot be maintained.[2]

Since the defocusing effect of the gaps is reduced by lowering the gap fields, and since the beam is then also handled more gently, one might expect reduced beam quality deterioration as a result. Another benefit is the reduced quadrupole gradients, which we have again determined from Figure 1. In Figure 5 we have plotted the variation of the ratio of final emittance to input emittance at a particlar final particle energy (7 MeV) with beam current. The curves for 80 percent of the particles are most representative as they discount the disproportionate contribution from a few particles. Results are given for gap fields of 5, 4 MV/m, and 2.5 MV/m. In the current range 15-25 mA, the relative emittance varies linearly with current. The proportionality constant ranges from 0.17 for a gap field of 5 MV/m to 0.023 for a gap field of 2.5 MV/m. In the latter case, therefore, the emittance gain is relatively independent of current.

In practice, the transverse excursions of the particles are limited by the bore size and the beam must be matched to the LINAC acceptance. To simulate this constraint, we have imposed an upper limit on the radius of

the beam, dropping particles if they exceed this value. An example is Figure 6 for which the initial current is 25 mA and the gap fields ≃ 2.5 MV/m. The radial cutoff is 2.5 cm and the curves indicate the axial positions at which particles are dropped. About 15 percent of the particles are lost. These include the losses from the "bucket." The increase in bunch length due to straggling particles is evident in Figure 6b. Thus, the transmitted current is about 20 mA for this case of gentle acceleration.

As the current is increased beyond 25 mA, there will come a point where a larger percentage is lost because the increase in the "bucket" size along the accelerator does not keep up with the spread due to longitudinal forces. The advantage of a larger separatrix fill factor would then be lost. Where this occurs depends on the initial distribution and to some extent on the details of the accelerating structure. These results indicate that it may be worthwhile to run at currents higher than the theoretical maximum and to use gradually increasing voltages in the first few gaps.

REFERENCES

1. T. Khoe, private communication.

2. J. W. Staples and R. A. Jameson, 1979 Particle Accelerator Conference NS26 No. 3 (San Francisco, March 1979).

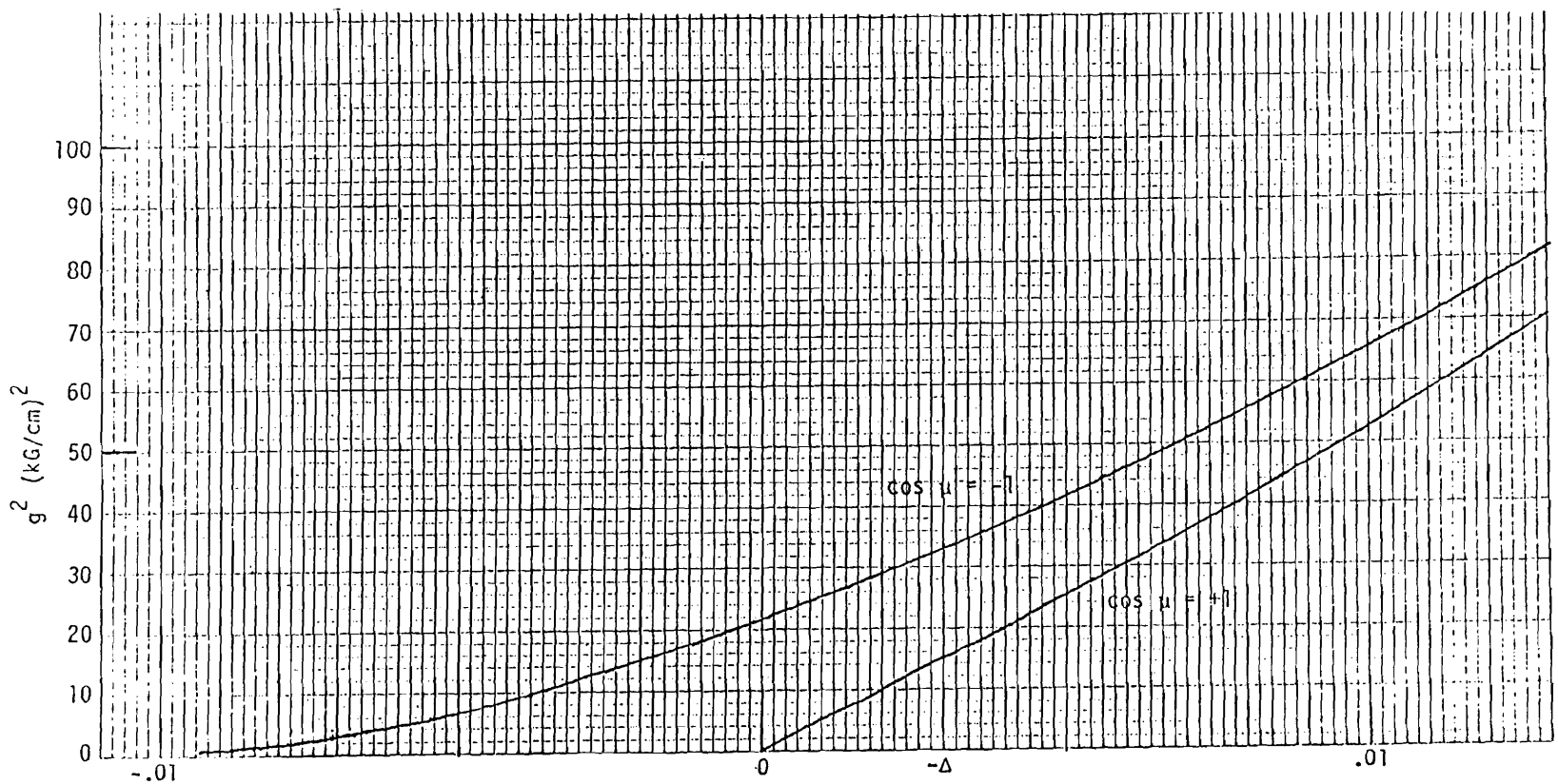

Figure 1. Magnetic Stability Limits for ++-- Geometry.

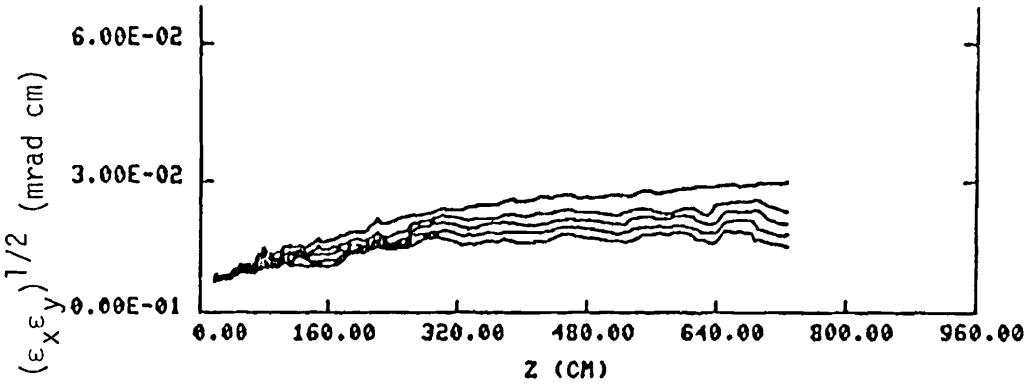

CASE = 09/20/79-004
I = 0.15000E-01
G = 0.51000E 01
AL1 = 0.10000E 01
ALPHA= 0.20000E 00
CCS = 0.69000E-06
C1 = 0.00000E 00
X = 0.18000E 01
XP = 0.29219E-02
Y = 0.70000E 00
YP = 0.75211E-02

Figure 2a. Mean Transverse Emittance

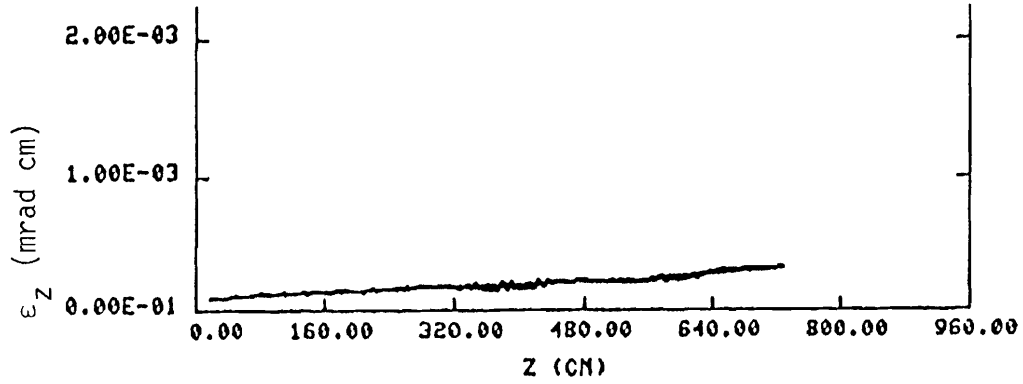

Figure 2b. Longitudinal Emittance

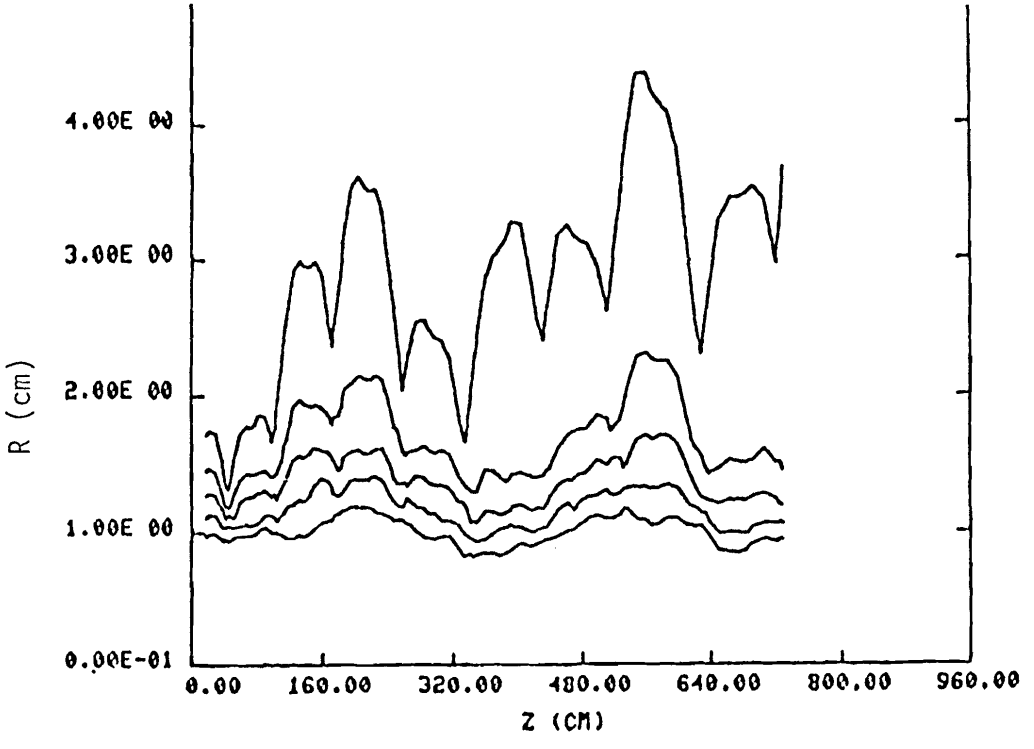

CASE = 09/20/79-004
I = 0.15000E-01
G = 0.51000E 01
AL1 = 0.10000E 01
ALPHA= 0.20000E 00
CCS = 0.69000E-06
C1 = 0.00000E 00
X = 0.18000E 01
XP = 0.29249E-02
Y = 0.70000E 00
YP = 0.75211E-02

Figure 2c. Beam Radius

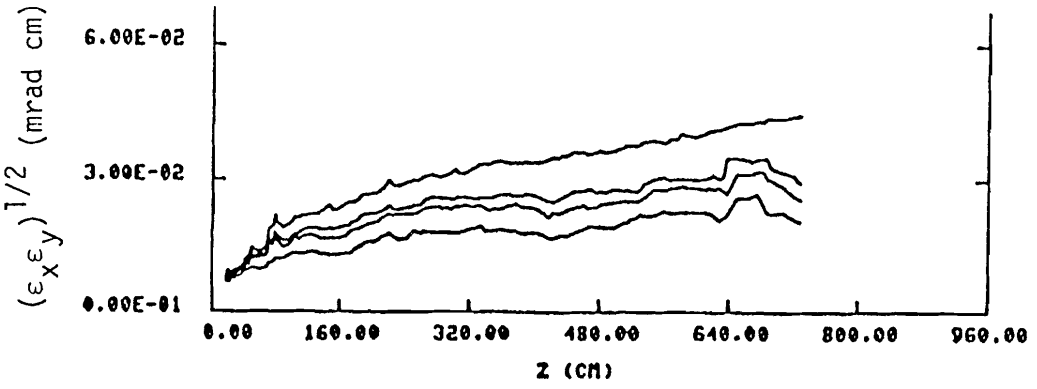

CASE • 09/12/79-004
I • 0.25000E-01
G • 0.51000E 01
AL1 • 0.10000E 01
ALPHA• 0.20000E 00
CCS • 0.69000E-06
C1 • 0.00000E 00
X • 0.21950E 01
XP • 0.23985E-02
Y • 0.93705E 00
YP • 0.56187E-02

Figure 3a. Mean Transverse Emittance

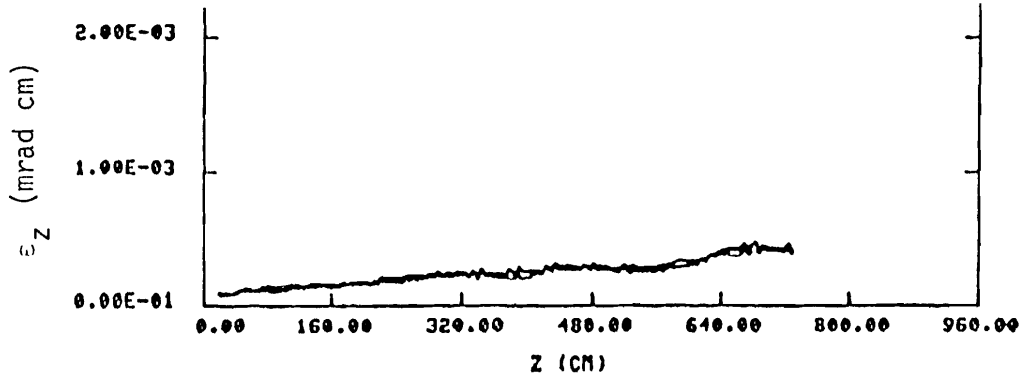

Figure 3b. Longitudinal Emittance

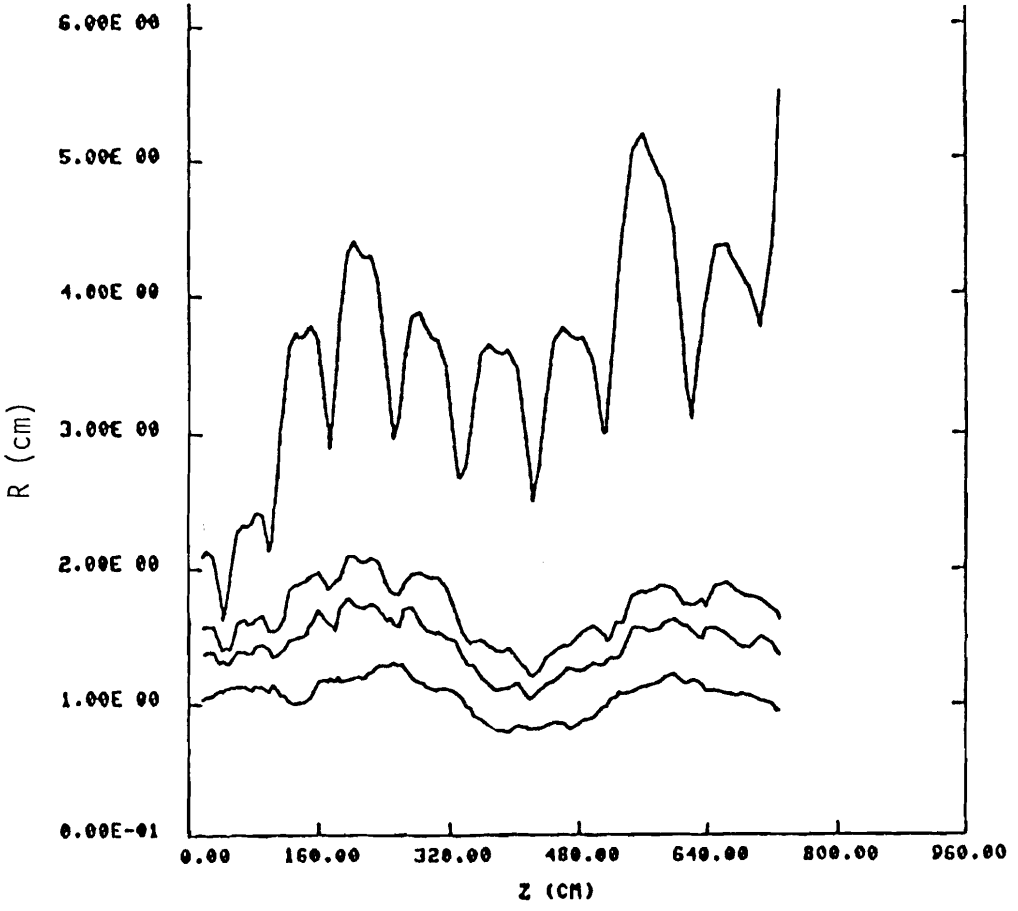

CASE = 09/12/79-004
I = 0.25000E-01
Q = 0.51000E 01
AL1 = 0.10000E 01
ALPHA= 0.20000E 00
CCS = 0.69000E-06
C1 = 0.00000E 00
X = 0.21950E 01
XP = 0.23985E-02
Y = 0.93705E 00
YP = 0.56187E-02

Figure 3c. Beam Radius

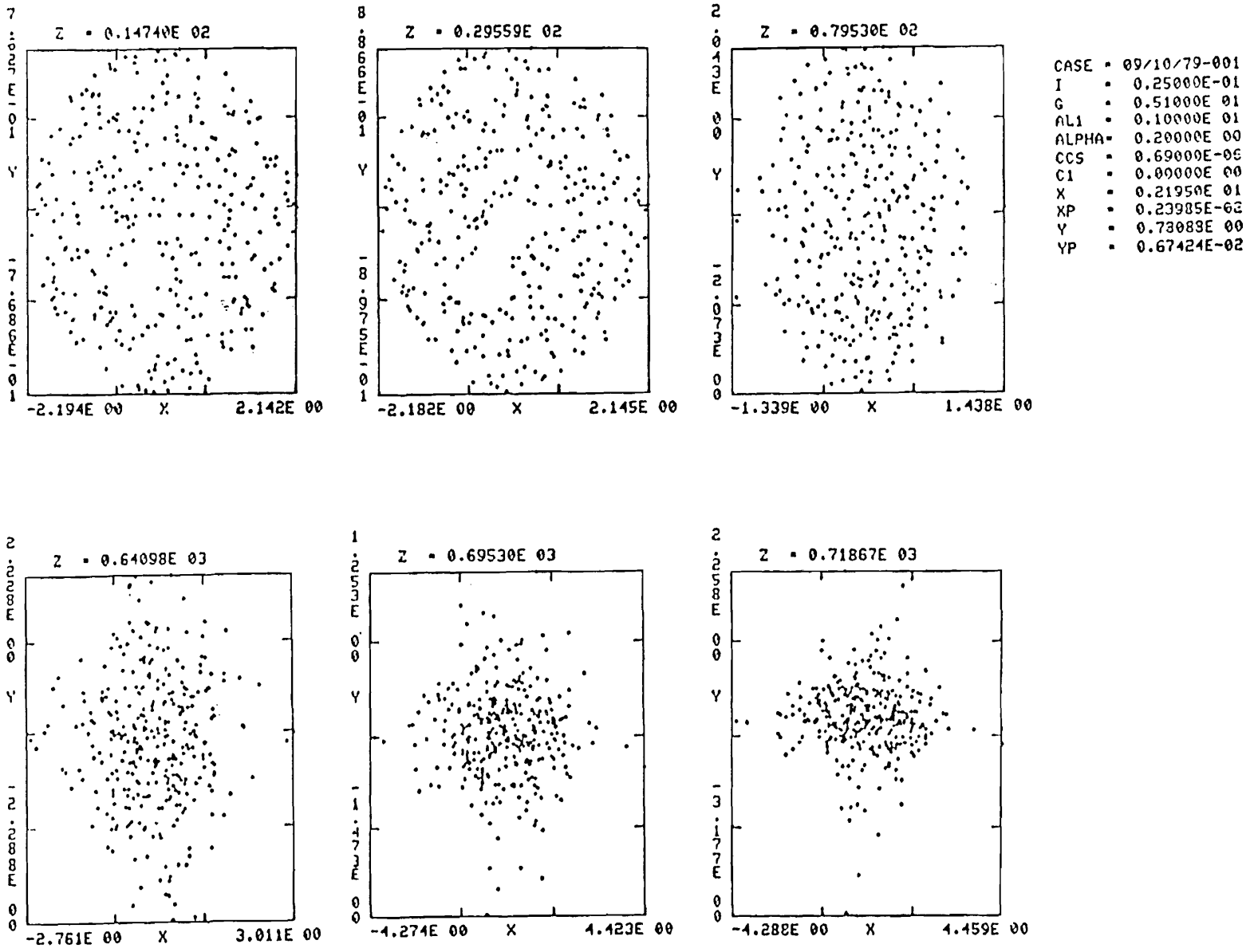

Figure 4.1. Space (x-y) Particle Distribution

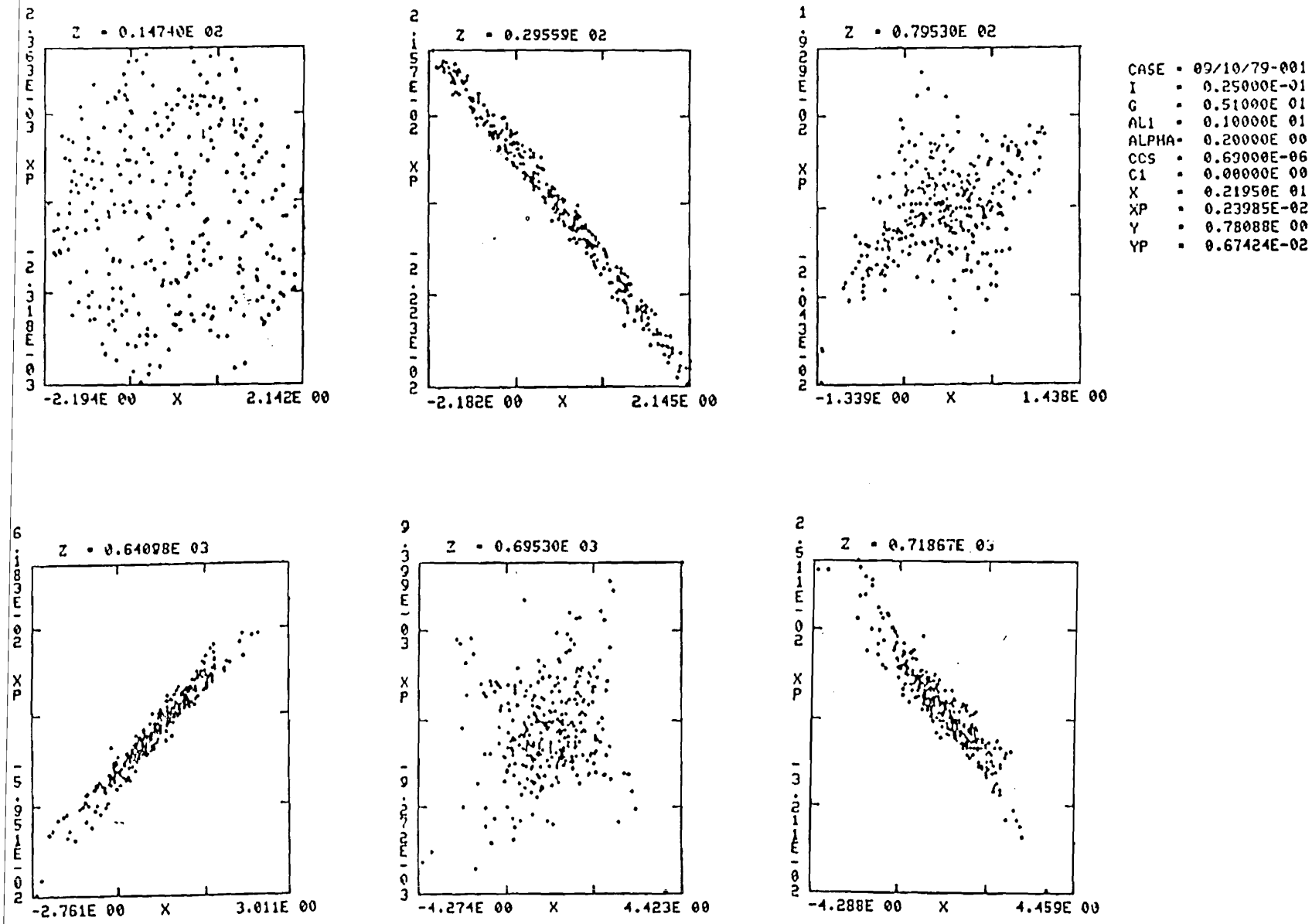

Figure 4.2. Phase-Space (x-xp) Particle Distribution

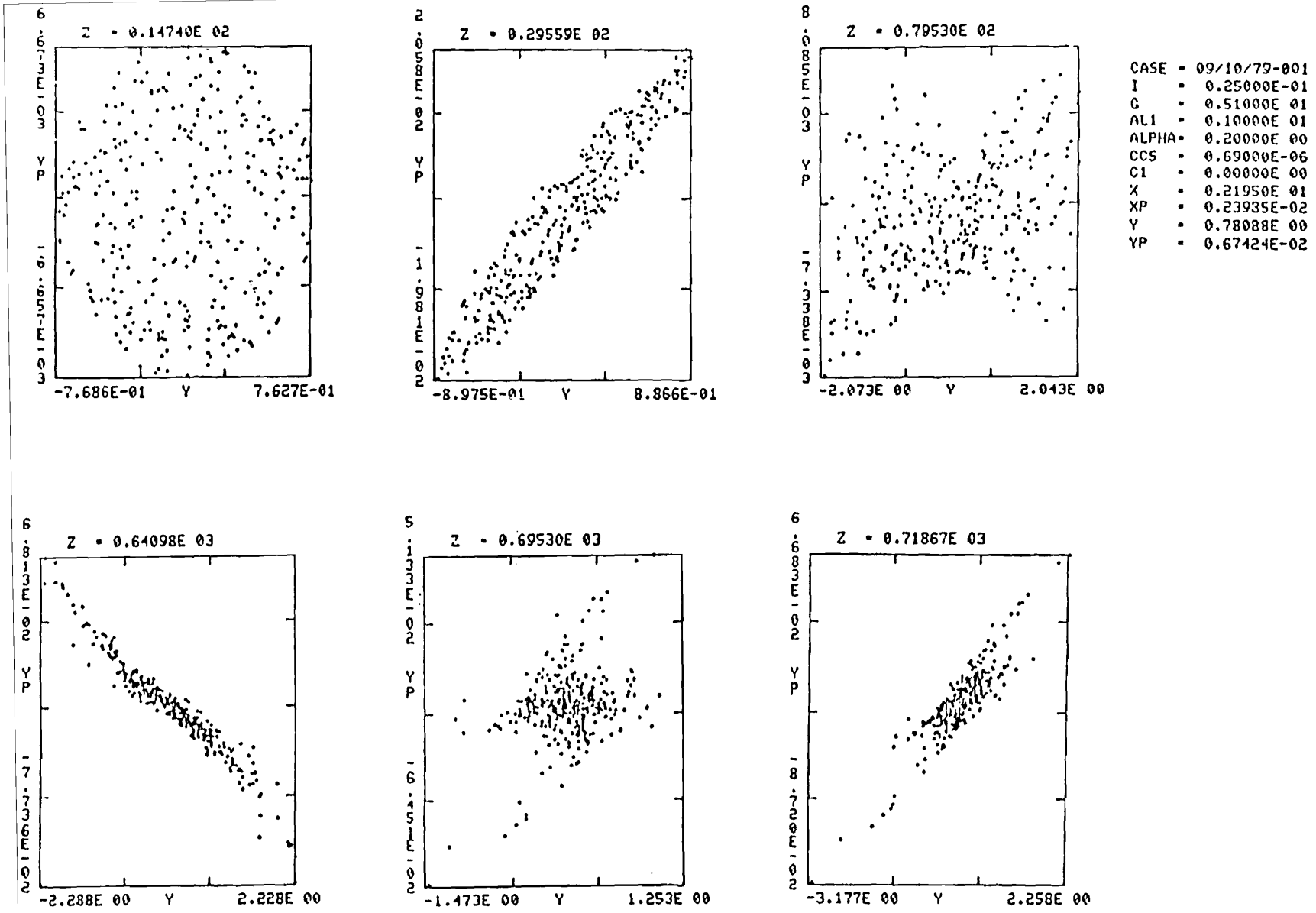

Figure 4.3. Phase-Space (y-yp) Particle Distribution

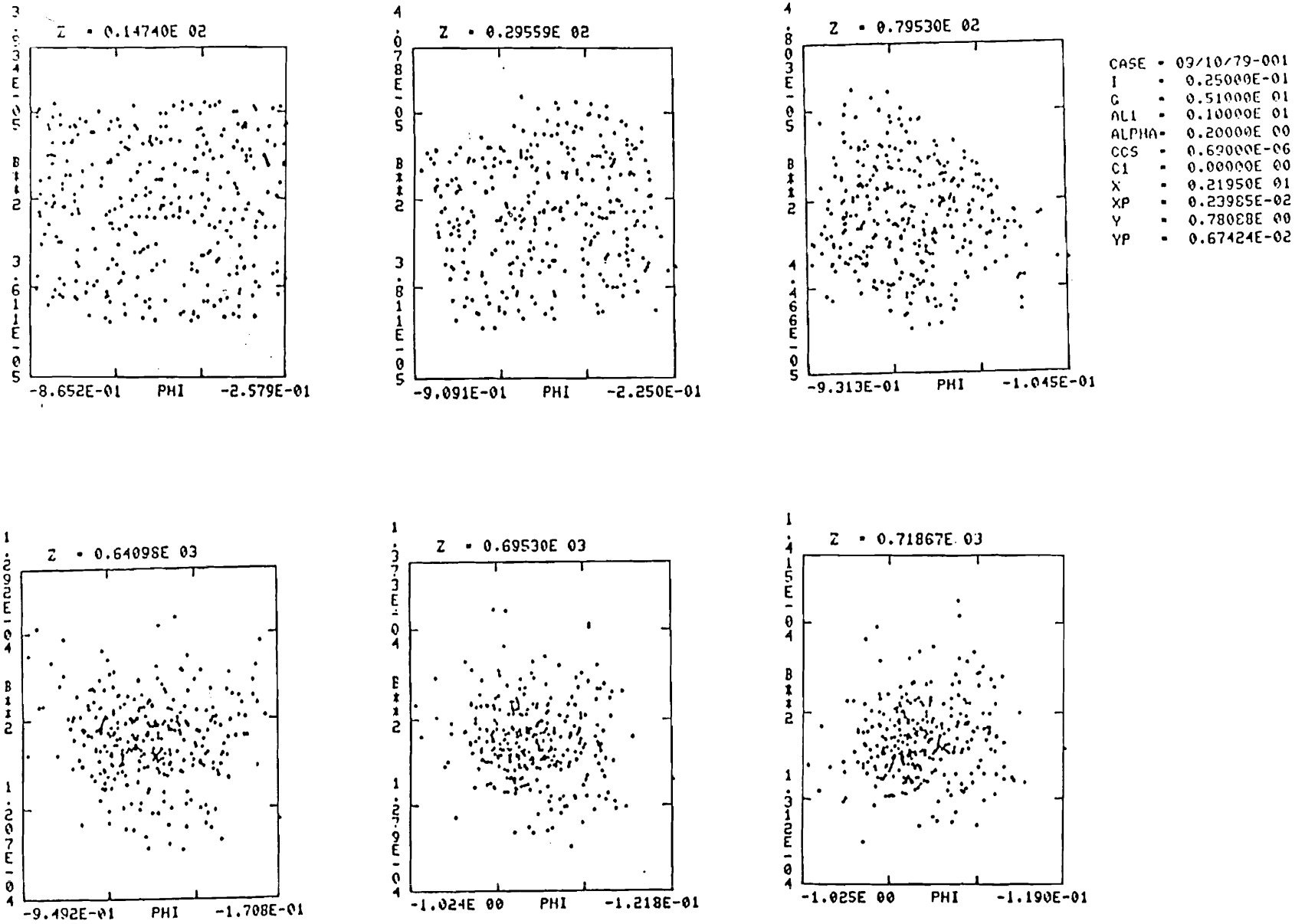

Figure 4.4. Phase-Space $((z-z_s) - (\beta-\beta_s))$ Particle Distribution

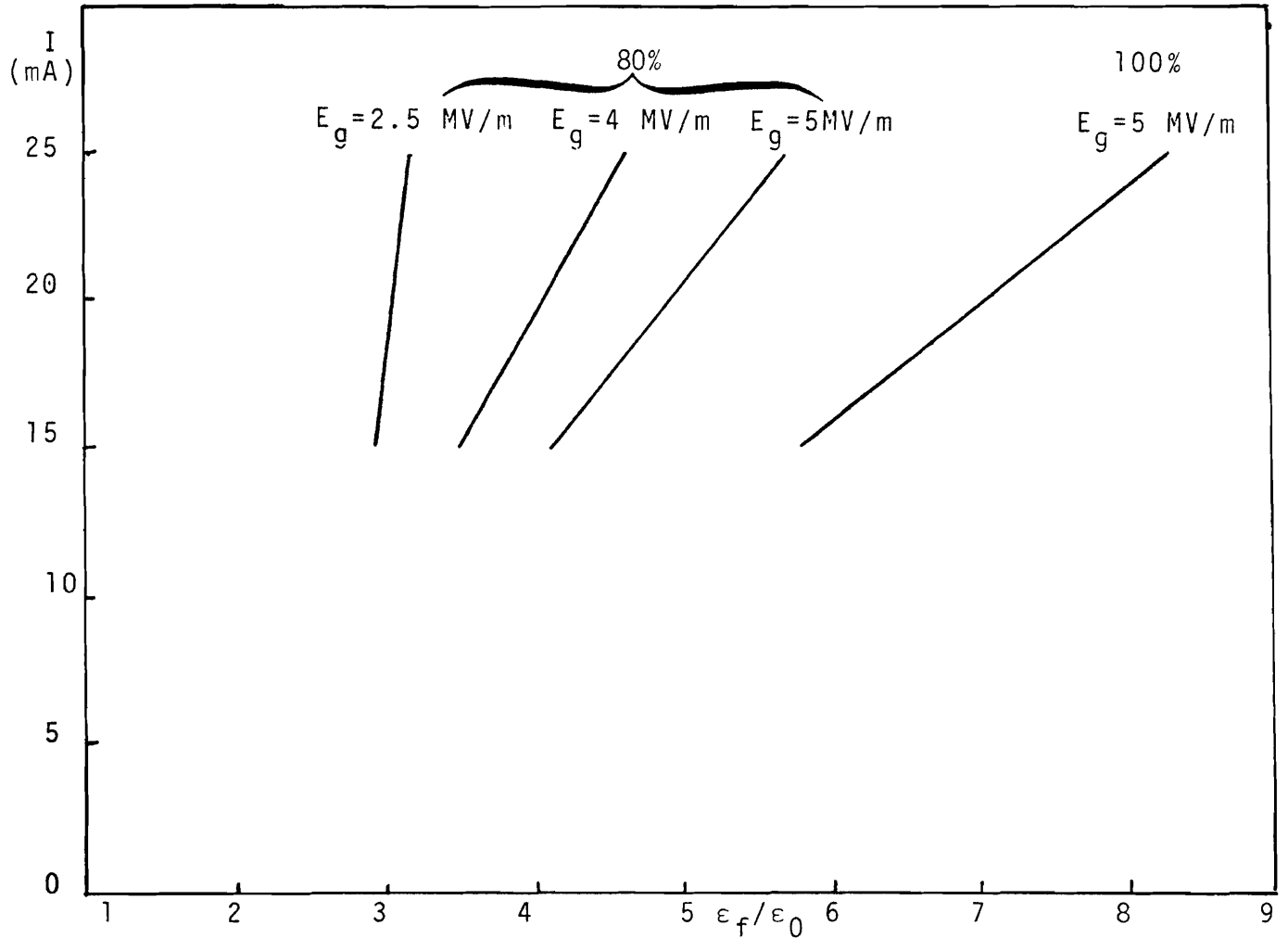

Figure 5. Emittance Variation with Current and Gap Field for Final Energy of 7 MeV.

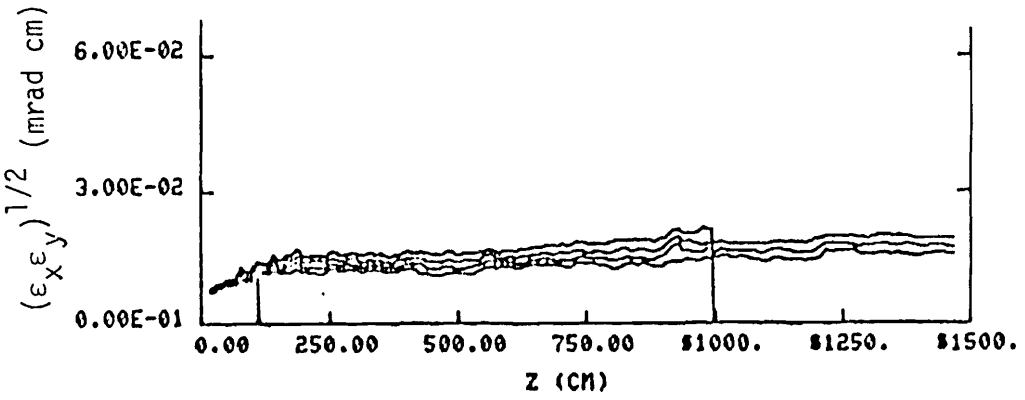

CASE = 10/02/79-001
I = 0.25000E-01
G = 0.43600E 01
AL1 = 0.10000E 01
ALPHA= 0.20000E 00
CCS = 0.34770E-06
C1 = 0.00000E 00
X = 0.18000E 01
XP = 0.29240E-02
Y = 0.85700E 00
YP = 0.61930E-02

Figure 6a. Mean Transverse Emittance

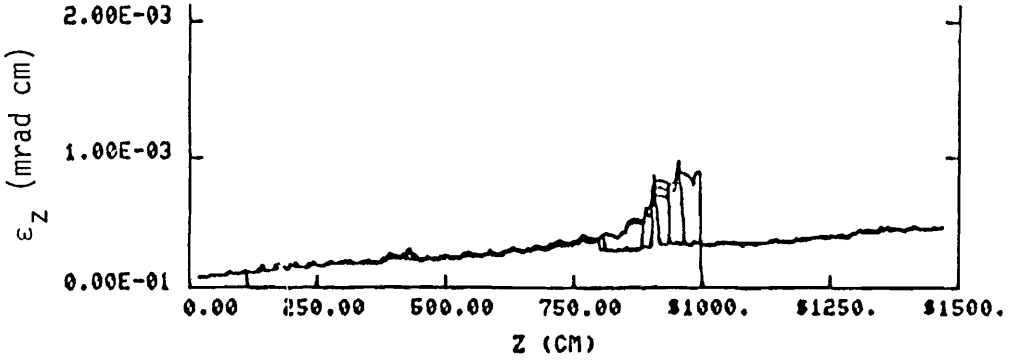

Figure 6b. Longitudinal Emittance

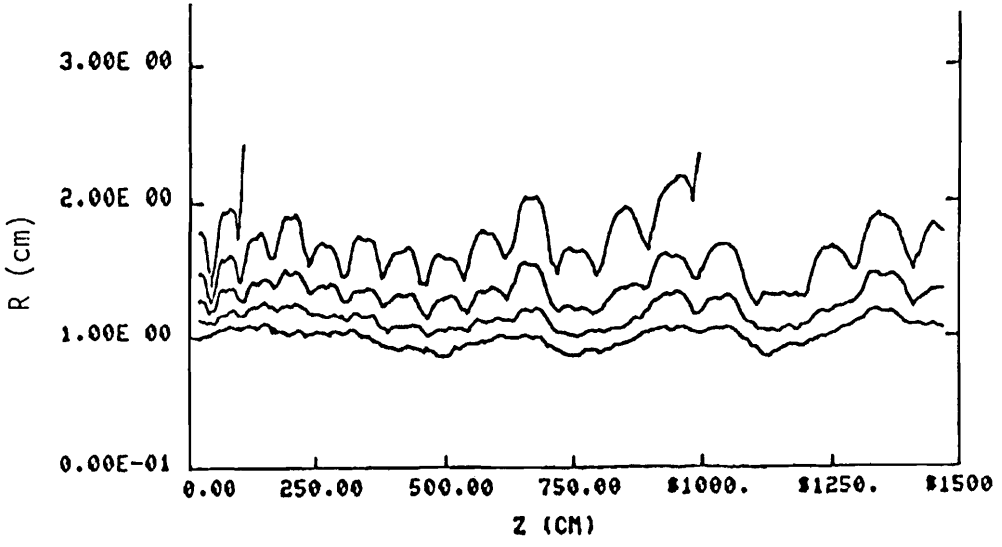

Figure 6c. Beam Radius

CASE = 10/02/79-001
I = 0.25000E-01
G = 0.43600E 01
AL1 = 0.10000E 01
ALPHA = 0.20000E 00
CCS = 0.34770E-06
C1 = 0.00000E 00
X = 0.18000E 01
XP = 0.29240E-02
Y = 0.85700E 00
YP = 0.61930E-02